

Optimization using Finite Element Models

Dehaeze Thomas

February 25, 2025

Contents

1	Reduced order flexible bodies	4
1.1	FEA Modal Reduction	4
1.2	Validation of the Method	5
2	Actuator	12
2.1	Choice of the Actuator based on Specifications	12
2.2	APA300ML - Reduced Order Flexible Body	14
2.3	Identification of the APA Characteristics	15
2.4	Simpler 2DoF Model of the APA300ML	16
2.5	Electrical characteristics of the APA	18
2.6	Validation with the Nano-Hexapod	19
3	Flexible Joint	21
3.1	Flexible joints for Stewart platforms	21
3.2	Bending and Torsional Stiffness	22
3.3	Axial Stiffness	24
3.4	Obtained design / Specifications	26
3.5	Validation with the Nano-Hexapod	27
	Bibliography	31

- In the detail design phase, one goal is to optimize the design of the nano-hexapod
- Parts are usually optimized using Finite Element Models that are used to estimate the static and dynamical properties of parts
- However, it is important to see how the dynamics of each part combines with the nano-hexapod and with the micro-station. One option would be to use a FEM of the complete NASS, but that would be very complex and it would be difficult to perform simulations of experiments with real time control implemented.
- The idea is therefore to combine FEM with the multi body model of the NASS. To do so, Reduced Order Flexible Bodies are used (Section 1)
 - The theory is described
 - The method is validated using experimental measurements
- Two main elements of the nano-hexapod are then optimized:
 - The actuator (Section 2)
 - The flexible joints (Section 3)

1 Reduced order flexible bodies

Goal:

- include parts from which dynamical properties are estimated from a FEM

Outline:

- Quick explanation of the theory
- Explain the implementation with FEA software (Ansys) and Simscape
- Experimental validation with an amplified piezoelectric actuator

[1] [2]

1.1 FEA Modal Reduction

- sub-components in the multi-body model as reduced order flexible bodies representing the component's modal behaviour with reduced mass and stiffness matrices obtained from finite element analysis (FEA) models
- matrices were created from FEA models via modal reduction techniques, more specifically the component mode synthesis (CMS).
- this makes this design approach a combined multibody-FEA technique.
- FEM: high number of DoF
- goal: reduce number of DoF, allow to integrate in multi-body simulation

Procedure:

- model the part in FE software as usually by defining material properties, etc.
- define frames for which we want to the multi-body model will then be able to interface with, and can be used to:
 - connect other parts
 - apply forces and torques
 - measure motion between frames

- perform the modal reduction technique from FEA (also called component mode synthesis or “Craig-Bampton” method) for the reduction of the high number of FEA degrees of freedom (DoF) to a smaller number of retained degrees of freedom typically from hundred thousands to less than 100 DoF
- the number of DoF is 6 times the number of defined frame + any number of additional DoF that we want to model $m = 6 \times n + p$ n the number of frames, p the number of additional modes
- then, it outputs $m \times m$ reduced mass and stiffness matrices
- in the multi-body model, the two reduced matrices can be used to model the part

1.2 Validation of the Method

Validation with Amplified Piezoelectric Actuator, because:

- is a good candidate for the nano-hexapod (as will be explained in Section 2)
- had one in the lab for experimental testing (APA95ML, Figure 1.1) It is composed of several piezoelectric stacks (arranged horizontally, in blue), and a shell (in red) that amplifies the motion. The working direction of the APA95ML is vertical.
- permits to model a mechanical structure (similar to a flexible joint), piezoelectric actuator and piezoelectric sensor

Quick explanation of APA:

- [3]

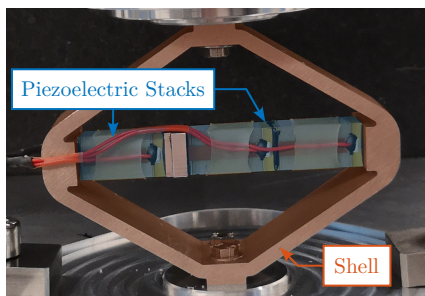


Figure 1.1: Picture of the APA95ML

Parameter	Unit	Value
Nominal Stroke	μm	100
Blocked force	N	1600
Stiffness	$N/\mu m$	16

Table 1.1: APA95ML specifications

Finite Element Model

- explain how the FEM is done:
 - material properties (Table 1.2)
 - mesh (Figure 1.2a)

- explain piezoelectric materials:
 - sensors
 - actuators
- choice of frames (Figure 1.2b)
 - 2 for each piezoelectric stack to measure strain and apply forces
 - 1 at the top, 1 at the bottom to connect to other elements
- choose number of DoF = i , size of model 7 frames + 6 modes = i order 48
- perform the reduction: show the output reduced matrices

Table 1.2: Material properties used for FEA modal reduction model. E is the Young’s modulus, ν the Poisson ratio and ρ the material density

	E	ν	ρ
Stainless Steel	190 GPa	0.31	7800 kg/m^3
Piezoelectric Ceramics (PZT)	49.5 GPa	0.31	7800 kg/m^3

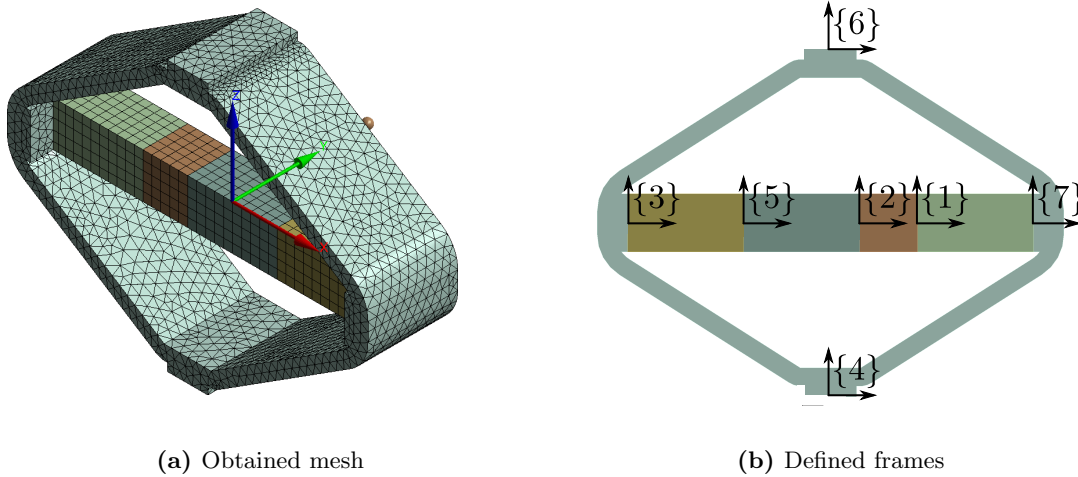


Figure 1.2: Finite element model of the APA95ML. Obtained mesh is shown in (a). Frames (or “remote points”) used for the modal reduction are shown in (b).

Super Element in the Multi-Body Model Model:

- Connect frame {4} to world frame and frame {6} to a 5.5kg mass, vertically guided
- 2 actuator stacks, 1 sensor stack:
 - force source between frames {3} and {2}
 - measured strain for force sensor by measuring the displacement between {1} and {7}

- Input: internal force applied
- Output: strain in the sensor stack
- Issue: how to convert voltage to force and strain to voltage?

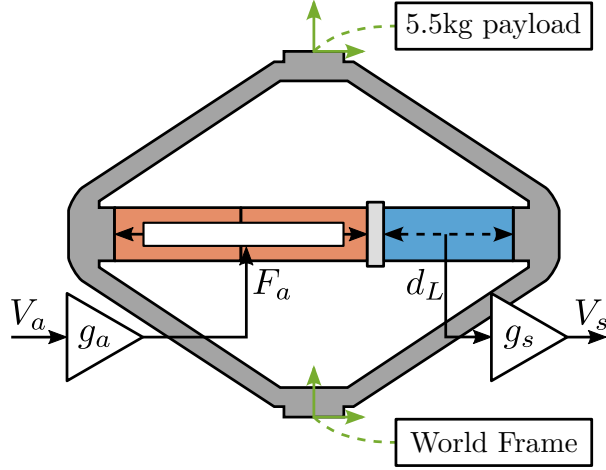


Figure 1.3: Amplified Piezoelectric Actuator Schematic

Need to link the electrical domain (voltages, charges) with the mechanical domain (forces, strain). To do so, “actuator constant” g_a and “sensor constant” g_s are used as shown in Figure 1.3.

A voltage V_a applied to the actuator stacks will induce an actuator force F_a :

$$F_a = g_a \cdot V_a \quad (1.1)$$

A change of length dl of the sensor stack will induce a voltage V_s :

$$V_s = g_s \cdot dl \quad (1.2)$$

In order to correctly model the piezoelectric actuator with Simscape, the values for g_a and g_s needs to be determined.

- g_a : the ratio of the generated force F_a to the supply voltage V_a across the piezoelectric stack
- g_s : the ratio of the generated voltage V_s across the piezoelectric stack when subject to a strain Δh

Sensor and Actuator “constants” The gains g_a and g_s were estimated from the physical properties of the piezoelectric stack material (summarized in Table 1.3).

From [4, p. 123], the relation between relative displacement d_L of the sensor stack and generated voltage V_s is given by (1.3a) and from [5] the relation between the force F_a and the applied voltage V_a is given by (1.3b).

Table 1.3: Stack Parameters

Parameter	Unit	Value
Nominal Stroke	μm	20
Blocked force	N	4700
Stiffness	$N/\mu m$	235
Voltage Range	V	-20 to 150
Capacitance	μF	4.4
Length	mm	20
Stack Area	mm^2	10x10

$$V_s = \underbrace{\frac{d_{33}}{\epsilon^T s^D n}}_{g_s} d_L \quad (1.3a)$$

$$F_a = \underbrace{d_{33} n k_a}_{g_a} \cdot V_a, \quad k_a = \frac{c^E A}{L} \quad (1.3b)$$

Unfortunately, it is difficult to know exactly which material is used in the amplified piezoelectric actuator¹. However, based on the available properties of the stacks in the data-sheet (summarized in Table 1.3), the soft Lead Zirconate Titanate “THP5H” from Thorlabs seemed to match quite well the observed properties. The properties of this “THP5H” material used to compute g_a and g_s are listed in Table 1.4.

From these parameters, $g_s = 5.1 V/\mu m$ and $g_a = 26 N/V$ were obtained.

Table 1.4: Piezoelectric properties used for the estimation of the sensor and actuators sensitivities

Parameter	Value	Description
d_{33}	$680 \cdot 10^{-12} m/V$	Piezoelectric constant
ϵ^T	$4.0 \cdot 10^{-8} F/m$	Permittivity under constant stress
s^D	$21 \cdot 10^{-12} m^2/N$	Elastic compliance understand constant electric displacement
c^E	$48 \cdot 10^9 N/m^2$	Young’s modulus of elasticity
L	20 mm per stack	Length of the stack
A	$10^{-4} m^2$	Area of the piezoelectric stack
n	160 per stack	Number of layers in the piezoelectric stack

Experimental Validation goal: validation of the procedure.

- Explain test bench: (Figure 1.4)
 - 5.7kg granite, vertical guided with an air bearing
 - fibered interferometer measured the vertical motion of the granite y

¹The manufacturer of the APA95ML was not willing to share the piezoelectric material properties of the stack.

- DAC generating control signal u , voltage amplifier gain of 20, V_a is the voltage across the two piezoelectric stacks
- ADC is used to measured the voltage across the piezoelectric sensor stack

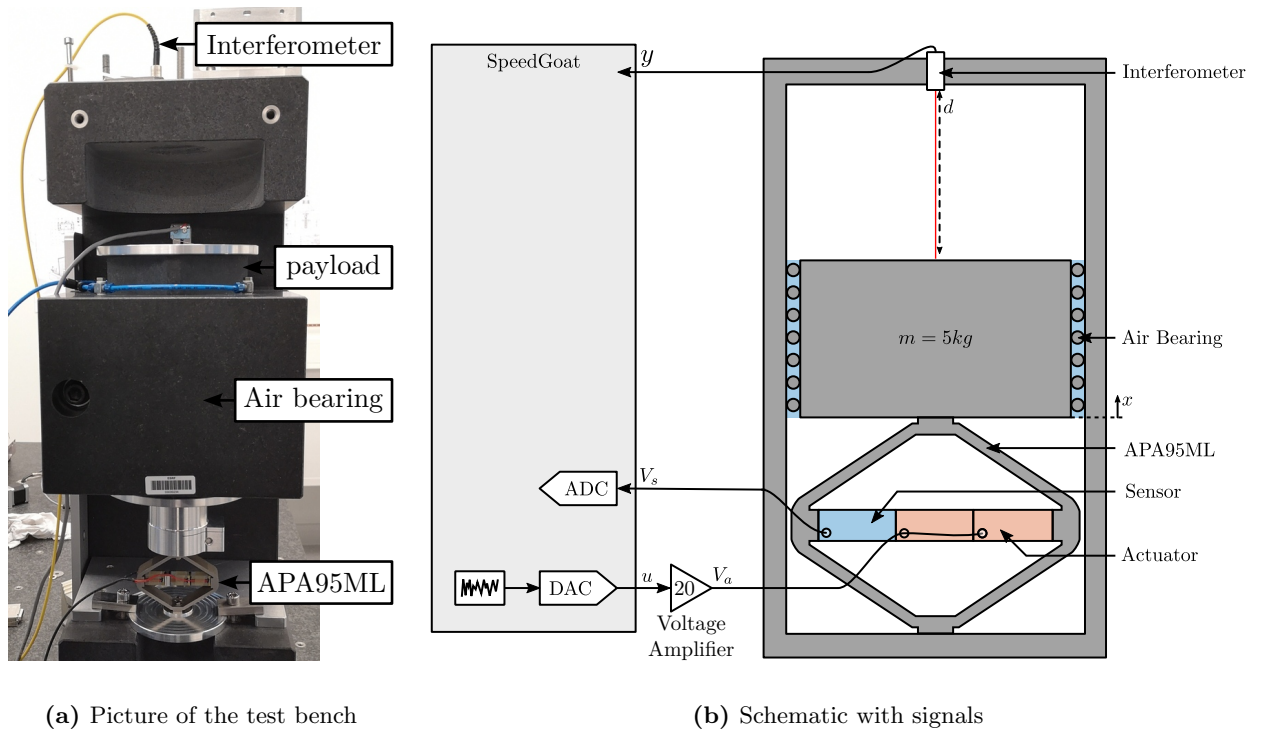


Figure 1.4: Test bench used to validate “reduced order solid bodies” using an APA95ML. Picture of the bench is shown in (a). Schematic is shown in (b).

- Explain how to experimentally measure the transfer function:
 - test signal, here noise
 - compute and show the transfer functions from V_a to y and to V_s
 - Compare the model and measurement: validation (Figure 1.5)
 - talk about the phase:
 - * for force sensor, just delay linked to the limited sampling rate of 0.1 ms
 - * for interferometer: additional delay due to electronics being used
 - good match. The gains can be further tuned based on the experimental results.
 - talk about minimum phase zero: will be discussed during the experimental phase

Integral Force Feedback with APA goal:

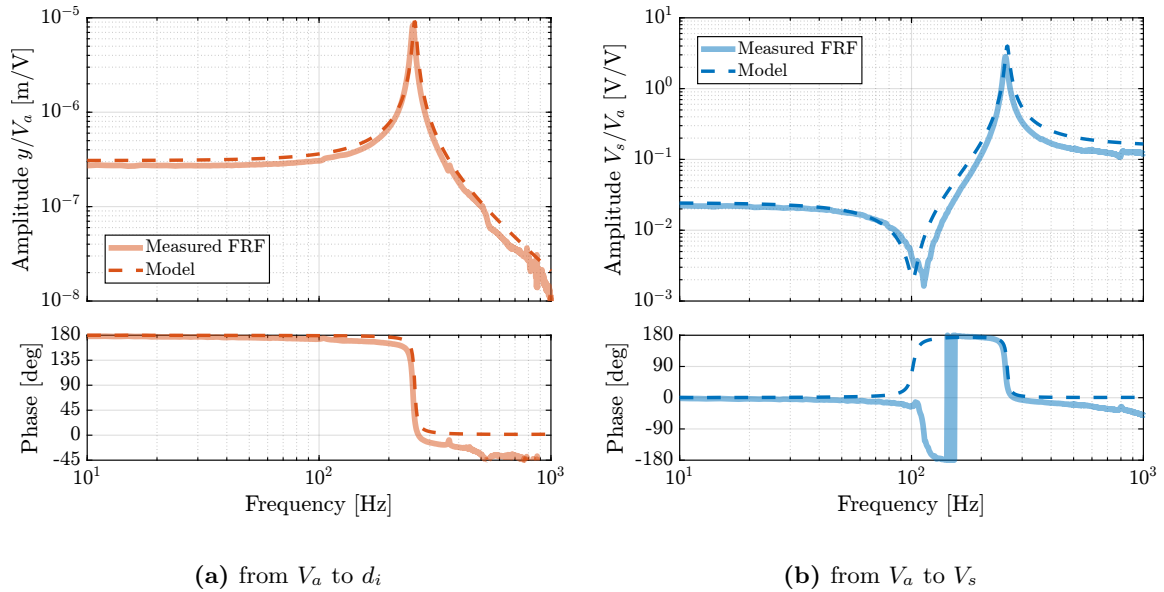


Figure 1.5: Comparison of the measured frequency response functions and the identified dynamics from the finite element model of the APA95ML. Both for the dynamics from V_a to d_i (a) and from V_a to V_s (b)

- validate the use of super element for control tasks

The controller used in the Integral Force Feedback Architecture is (1.4), with g a gain that can be tuned.

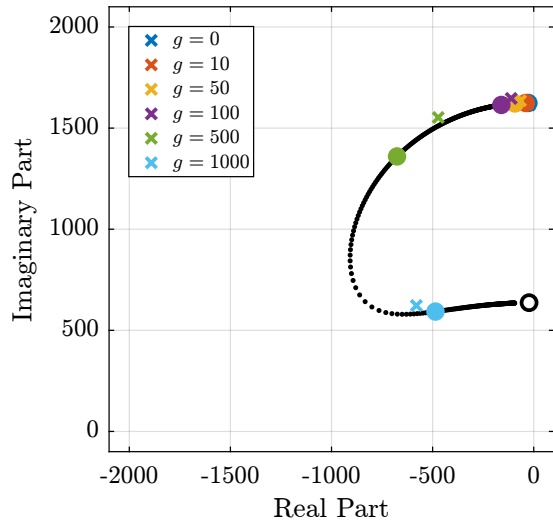
$$K_{\text{IFF}}(s) = \frac{g}{s + 2 \cdot 2\pi} \cdot \frac{s}{s + 0.5 \cdot 2\pi} \quad (1.4)$$

Above 2 Hz the controller is basically an integrator, whereas an high pass filter is added at 0.5Hz to further reduce the low frequency gain. In the frequency band of interest, this controller should mostly act as a pure integrator.

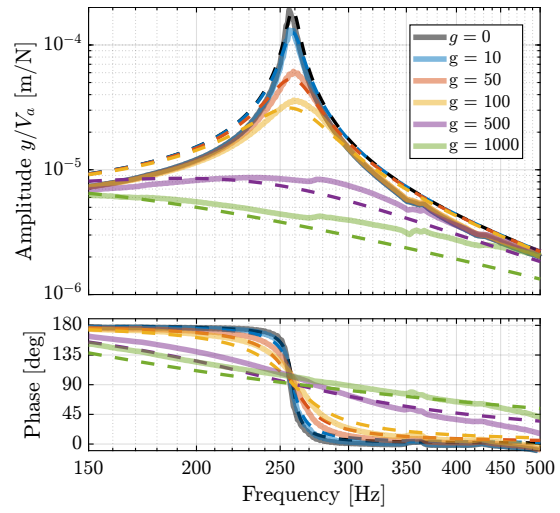
Maybe make a block diagram of the control with added damped input

Conclusion

- Validation of the method
- Very useful to optimize different parts
- However, model order may become very large and not convenient to perform time domain simulations
- But extracting dynamics is not computational intensive, even for large model orders



(a) Root Locus plot



(b) Damped plants

Figure 1.6: Obtained results using Integral Force Feedback with the APA95ML.

- For instance APA: order 48, 6 APA for the nano hexapod 288 orders just for the APA
[published paper](#)

2 Actuator

Goals:

- Based on dynamical models and previous studies, extract specifications for the actuators to be included in the nano-hexapod. Then choose the most appropriate actuator based on specifications (Section 2.1)
- Model this actuator accurately using a “reduced order flexible body” to check the dynamics and validate the choice of actuator and validate this choice with simulations
- Development of a 2DoF model for lower order models (i.e. for simulations)

2.1 Choice of the Actuator based on Specifications

From previous analysis:

- Actuator stiffness has major impact on the system dynamics and performances due to several factors:
 - Spindle rotation: modification of plant dynamics and coupling increase due to Gyroscopic effects This require to have stiffness above \sim
 - Limited micro-station compliance / complex dynamics: The actuator stiffness should be small enough such that the suspension modes of the nano-hexapod are below the problematic modes of the micro-stations.
 - There is therefore an intermediate stiffness that is foreseen to give the best compromise, and it is around $1\text{ N}/\mu\text{m}$
- HAC-LAC strategy: Actuator must include a force sensor Because of the rotation, some stiffness should be present in parallel to the force sensor
- Limited space: As the maximum height of the nano-hexapod is 95mm, and each strut has a flexible joint at each end, it is estimated that the maximum height of the actuator should be less than 50mm
- Stroke: The stroke of the each actuator should be large enough such that the nano-hexapod mobility exceed the micro-station positioning errors. Some margins should be included for mounting errors, and further flexibility of the system (for instance to perform scans with the nano-hexapod, or to align the point of interest with the rotation axis)

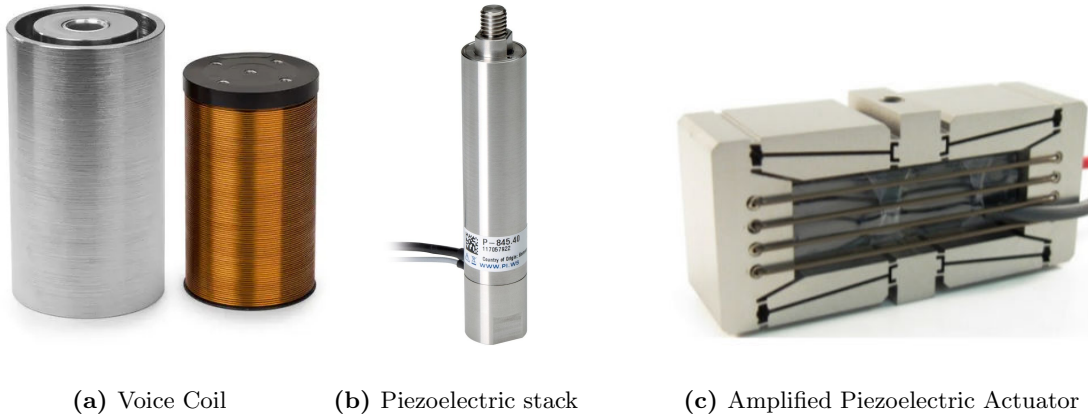
Actuator specifications:

- Height ($\approx 50\text{mm}$)
- Stroke ($\sim 100\mu\text{m}$)
- Stiffness ($0.1\text{--}1\text{ N}/\mu\text{m}$)
- Blocked force?
- Force sensor

Options:

- Two main options: piezoelectric actuators and Lorentz actuator (also known as Voice coil actuators). Variable reluctance actuators were not considered, even though they have better efficiency than voice coil actuators, they are non linear and induce additional control complexity.
- Voice coil + relatively soft flexible guiding ($1\text{N}/\mu\text{m}$):
 - required force $\sim 100\text{N}$ for $100\mu\text{m}$ correction This constant force/current would induce large thermal loads, that may negatively impact system's stability Advantages of voice coil (longer strokes than piezo + allow for very low stiffness in the direction of actuation, extremely linear for high performance feedforward) are not used here.
- Piezoelectric stack actuators:
 - PZT: stroke $\sim 0.1\%$ of its length.
 - 50mm length $\Rightarrow 50\mu\text{m}$ stroke which is barely enough
 - Extremely stiff, in the order of $100\text{ N}/\mu\text{m}$, which is not wanted here.
- Amplified Piezoelectric Actuator:
 - shell is used to pre-stress the piezoelectric stacks and amplify the motion (roughly by the ratio of the width over the height)
 - This also reduce the stiffness in the direction of motion
 - This make this design quick compact in the direction of motion (i.e. in height)
 - When several stacks are used, one of them can be used as a force sensor, which is therefore very well collocated with the actuators
 - Therefore, this actuator is well suited for decentralized IFF, already applied for a Stewart platform with APA [6]

Based on previous analysis, it was decided to use amplified piezoelectric actuators for the nano-hexapod. Table 2.1: compares few models that fulfill specifications. It was decided to go for the APA300ML (shown in Figure 2.2a). One reason is that we already had experience with APA from Cedrat technologies, and the Finite Element Model was validated experimentally, so we are confident to model the APA300ML with FEA and include it in the NASS model for validation.



(a) Voice Coil (b) Piezoelectric stack (c) Amplified Piezoelectric Actuator

Figure 2.1: Example of actuators considered for the nano-hexapod. Voice coil from Sensata Technologies (a). Piezoelectric stack actuator from Physik Instrumente (b). Amplified Piezoelectric Actuator from DSM (c).

- Talk about piezoelectric actuator? bandwidth? noise?
- Resolution: really depends on the electrical noise (induced by DAC and voltage amplifier). They will be chosen appropriately

Table 2.1: List of some amplified piezoelectric actuators that could be used for the nano-hexapod

Specification	APA150M	APA300ML	APA400MML	FPA-0500E-P	FPA-0300E-S
Stroke $> 100 [\mu m]$	187	304	368	432	240
Stiffness $\approx 1 [N/\mu m]$	0.7	1.8	0.55	0.87	0.58
Resolution $< 2 [nm]$	2	3	4		
Blocked Force $> 100 [N]$	127	546	201	376	139
Height $< 50 [mm]$	22	30	24	27	16

2.2 APA300ML - Reduced Order Flexible Body

To validate the choice of the APA300ML (Shown in Figure 2.2a):

- the APA300ML is modeled using a Finite Element Software
- a *super element* is exported and imported in Simscape where its dynamic is studied
- similarly to what was done with the APA95ML, frames defined for the *super element* are shown in figure 2.2b
- For this reduced order model, 7 frames are defined and 120 additional modes are modelled for a total matrix size of 162.
- This is very large and will not be practical for simulations, but the best model accuracy was wanted for validation
- The blue frames are used to model the force sensor stack: the relative motion between the two frame is measured

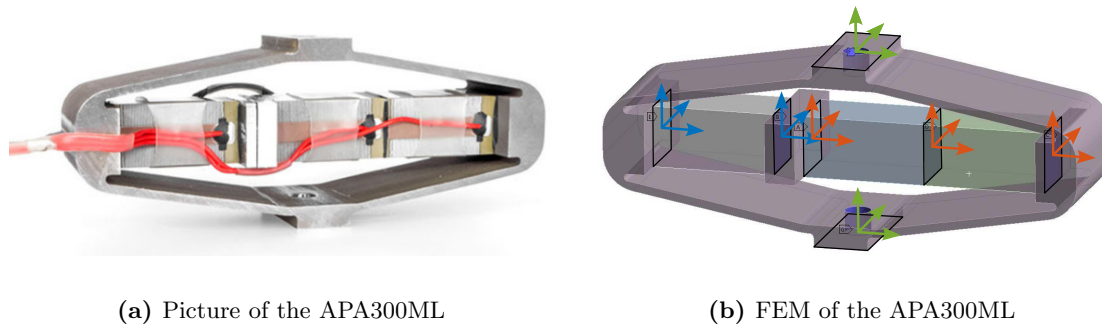


Figure 2.2: Amplified Piezoelectric Actuator APA300ML. Picture shown in (a). Frames (or “remote points”) used for the modal reduction are shown in (b).

- The red frames are used to model the two actuator stacks: *internal force* are added
- One mass is fixed at one end of the piezo-electric stack actuator (remove point F), the other end is fixed to the world frame (remote point G).
- The link between mechanical properties and electrical properties was discussed in Section 1.2. As the stacks are the same between the APA300ML and the APA95ML, the values estimated for g_a and g_s are used for the APA300ML.

2.3 Identification of the APA Characteristics

A first validation of the FEM and inclusion of the “reduced order flexible model” in the multi body-model is performed by computed some key characteristics of the APA that can be compared against the datasheet.

Stiffness The stiffness is estimated by extracting the transfer function from a vertical force applied on the top frame to the displacement of the same top frame. The inverse of the DC gain this transfer function should be equal to the axial stiffness of the APA300ML. A value of $1.75 N/\mu m$ is found which is close to the specified stiffness in the datasheet of $k = 1.8 N/\mu m$. See compliance transfer function 2.3.

Resonance Frequency The resonance frequency in the block-free condition is specified to be between 650Hz and 840Hz. This is estimated at 709Hz from the model (Figure 2.3).

Amplification Factor and Actuator Stroke The amplification factor is the ratio of the vertical displacement to the (horizontal) stack displacement. It can be estimated from the multi-body model by computing the transfer function from the horizontal motion of the stacks to the vertical motion of the APA. The ratio between the two is found to be equal to 5. This is linked to the

From the data-sheet of the piezoelectric stacks (see Table 1.3, page 8), the nominal stroke of the stack is $20 \mu m$ (which is typical for PZT to have a maximum stroke equal to 0.1 % of its length, here equal to $20 mm$). Three stacks are used, for an horizontal stroke of the stacks of $60 \mu m$. With an amplification

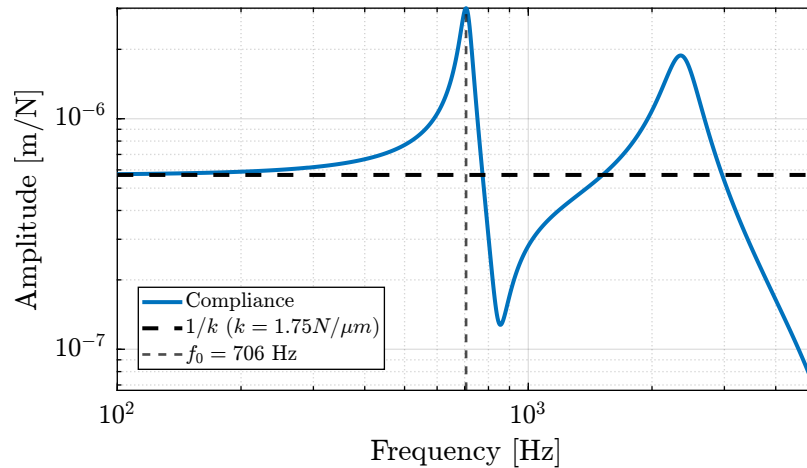


Figure 2.3: Estimated compliance of the APA300ML

factor equal to 5, the vertical stroke is estimated at $300 \mu\text{m}$, which corresponds to what is indicated in the datasheet.

This analysis provides some confidence on the model accuracy.

2.4 Simpler 2DoF Model of the APA300ML

- *super-element* order is quite large, and therefore not practical for simulations
- the goal here is to develop a low order model, that still represents wanted characteristics of the APA300ML:
 - axial stiffness
 - actuator and force sensor characteristics
- what is not modelled:
 - higher order modes
 - the flexibility of the APA in the other directions
- Therefore this model can be useful for simulations as it contains a very limited number of states, but when more complex dynamics of the APA is to be modelled, a flexible model will be used.

2DoF Model The model is adapted from [7].

It can be decomposed into three components:

- the shell whose axial properties are represented by k_1 and c_1

- the actuator stacks whose contribution to the axial stiffness is represented by k_a and c_a . The force source f represents the axial force induced by the force sensor stacks. The sensitivity g_a (in N/m) is used to convert the applied voltage V_a to the axial force f
- the sensor stack whose contribution to the axial stiffness is represented by k_e and c_e . A sensor measures the stack strain d_e which is then converted to a voltage V_s using a sensitivity g_s (in V/m)

Such a simple model has some limitations:

- it only represents the axial characteristics of the APA as it is modeled as infinitely rigid in the other directions
- some physical insights are lost, such as the amplification factor and the real stress and strain in the piezoelectric stacks
- the creep and hysteresis of the piezoelectric stacks are not modeled as the model is linear

The main advantage is that this model is very simple, only adds 4 states

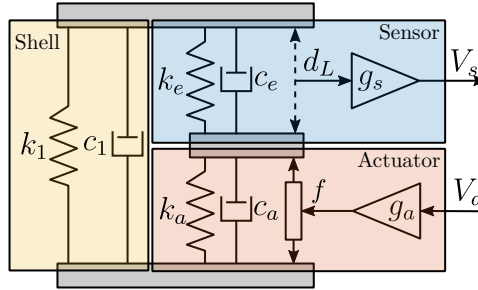


Figure 2.4: Schematic of the 2DoF model of the Amplified Piezoelectric Actuator

Parameter Tuning 9 parameters (m , k_1 , c_1 , k_e , c_e , k_a , c_a , g_s and g_a) have to be tuned such that the dynamics of the model (Figure 2.4) well represents the identified dynamics using the FEM.

- Mass is 5kg (similar to the test bench)
- Tune the parameters:
 - From the first zero of the transfer function from V_a to V_s , k_1 and c_1 are tuned
 - From the first pole of the transfer function from V_a to y , k_a , c_a , k_e , c_e are tuned
 - because the actuator and sensor stacks are physically the same, we suppose Then, it is reasonable to assume that the sensor stacks and the two actuator stacks have identical mechanical characteristics. Therefore, we have $k_e = 2k_a$ and $c_e = 2c_a$ as the actuator stack is composed of two stacks in series.
 - In the last step, g_s and g_a for the 2DoF motion can be tuned to match the gain of the transfer functions extracted from the FEM
 - Found parameters are summarized in Table 2.2

- Comparison of the transfer functions extracted from the high order flexible model with the 4th order (2DoF) model is done in Figure 2.5. Good match is obtained. Of course, higher order modes are not represented by the 2DoF model, nor the limited stiffness in the other directions.

Table 2.2: Summary of the obtained parameters for the 2 DoF APA300ML model

Parameter	Value
k_1	$0.30 \text{ N}/\mu\text{m}$
k_e	$4.3 \text{ N}/\mu\text{m}$
k_a	$2.15 \text{ N}/\mu\text{m}$
c_1	$18 \text{ Ns}/\text{m}$
c_e	$0.7 \text{ Ns}/\text{m}$
c_a	$0.35 \text{ Ns}/\text{m}$
g_a	$2.7 \text{ N}/\text{V}$
g_s	$0.53 \text{ V}/\mu\text{m}$

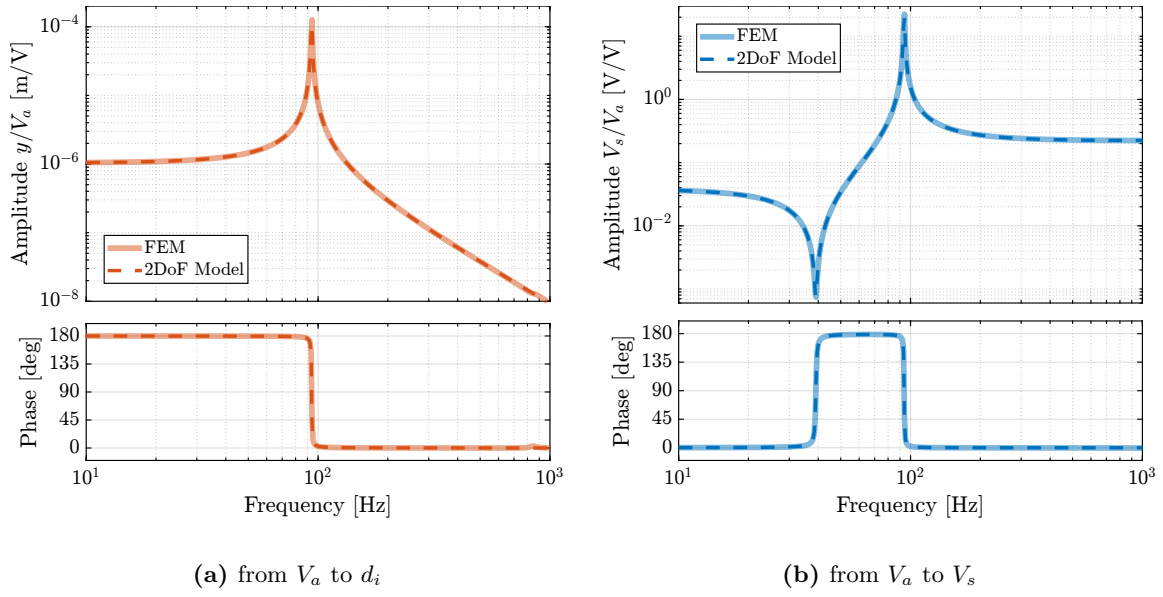


Figure 2.5: Comparison of the transfer functions extracted from the finite element model of the APA300ML and of the 2DoF model. Both for the dynamics from V_a to d_i (a) and from V_a to V_s (b)

2.5 Electrical characteristics of the APA

- Mechanical equations and electrical equations are coupled
- This means for instance, that the stiffness of the piezoelectric stack (i.e. the APA) depends on the electrical boundaries of the stacks:
 - Short circuited stacks are less stiff than open-circuited ones
 - This effect is quite small: example with the APA95ML (Figure 2.6) transfer function from V_a to d_i are estimated with the force sensor stack being short circuited or open-circuited.

- In the model used, the electrical phenomena are not modelled. But as this effect is small, it should be fine
- The electrical characteristics of the APA are very important both from the voltage amplifier side and the ADC measuring the force sensor voltage. This will be discussed in chapter “instrumentation”

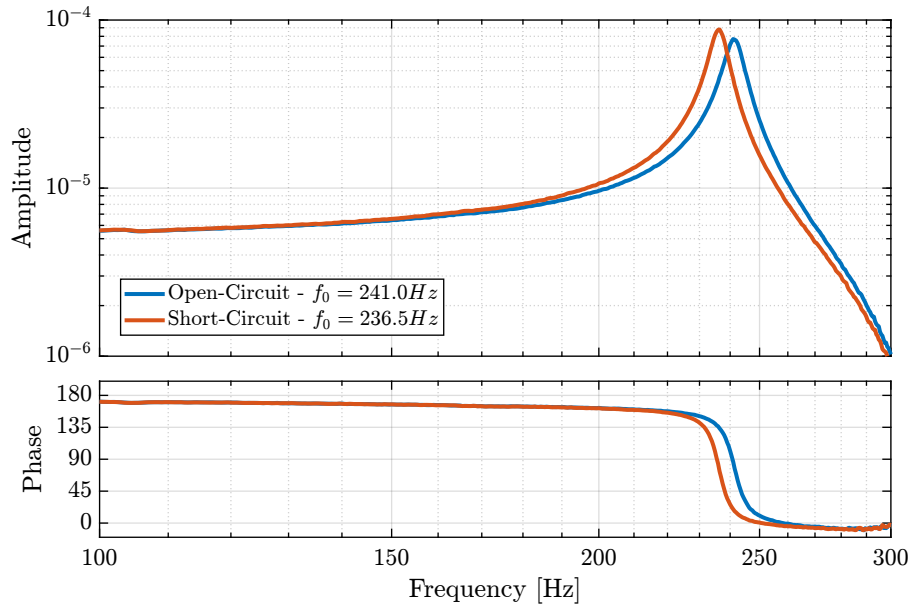
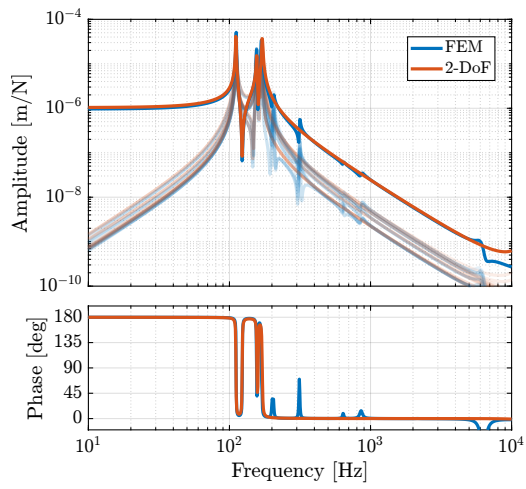


Figure 2.6: Effect of the electrical boundaries of the force sensor stack on the APA95ML resonance frequency

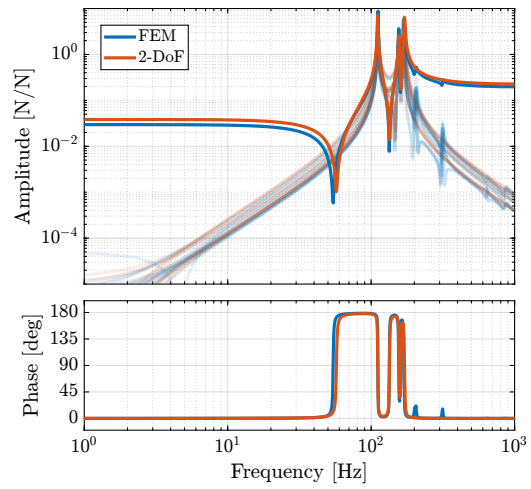
2.6 Validation with the Nano-Hexapod

NASS model + FEM model (or just 2DoF) of APA300ML = ζ validation (based on what?)

- Compare 2DoF model and FEM (Figure 2.7)
 - HAC plant
 - IFF Plant
 - Very similar = ζ can use 2nd order actuator models
- Talk about model order
 - 2DoF actuators: 24 states
 - FEM actuators: here matrices have a size of $36 \times 36 + 12 = \zeta \sim 300$



(a) f to $\epsilon_{\mathcal{L}}$



(b) f to f_m

Figure 2.7: Comparison of the dynamics obtained between a nano-hexpod having the actuators modelled with FEM and a nano-hexapod having actuators modelled a 2DoF system. Both from actuator force f to strut motion measured by external metrology $\epsilon_{\mathcal{L}}$ (b) and to the force sensors f_m (a).

3 Flexible Joint

The flexible joints have few advantages compared to conventional joints such as the **absence of wear, friction and backlash** which allows extremely high-precision (predictable) motion. The parasitic bending and torsional stiffness of these joints usually induce some **limitation on the control performance**. [8]

In this document is studied the effect of the mechanical behavior of the flexible joints that are located the extremities of each nano-hexapod's legs.

Ideally, we want the x and y rotations to be free and all the translations to be blocked. However, this is never the case and we have to consider:

- Non-null bending stiffnesses
- Non-null radial compliance
- Axial stiffness in the direction of the legs

This may impose some limitations, also, the goal is to specify the required joints stiffnesses.

Say that for simplicity (reduced number of parts, etc.), we consider the same joints for the fixed base and the top platform.

Outline:

- Perfect flexible joint
- Imperfection of the flexible joint: Model
- Study of the effect of limited stiffness in constrain directions and non-null stiffness in other directions
- Obtained Specification
- Design optimisation (FEM)
- Implementation of flexible elements in the Simscape model: close to simplified model

3.1 Flexible joints for Stewart platforms

Review of different types of flexible joints for Stewart platforms (see Figure 3.1).

Typical specifications:

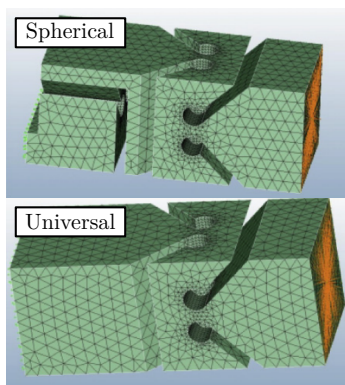
- Bending stroke (i.e. long life time by staying away from yield stress, even at maximum deflection/load)
- Axial stiffness
- Bending stiffness
- Maximum axial load
- Well defined rotational axes

Typical values?

- $K_{\theta,\phi} = 15 [Nm/rad]$ stiffness in flexion
- $K_{\psi} = 20 [Nm/rad]$ stiffness in torsion
-

$$K_a = 60 [N/\mu m]$$

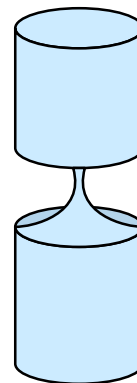
axial stiffness



(a)



(b)



(c)

Figure 3.1: Example of different flexible joints geometry used for Stewart platforms. (a) [9]. (b) [10]. (c) [11].

3.2 Bending and Torsional Stiffness

Because of bending stiffness of the flexible joints, the forces applied by the struts are no longer aligned with the struts (additional forces applied by the “spring force” of the flexible joints).

In this section, we wish to study the effect of the rotation flexibility of the nano-hexapod joints.

- To simplify the analysis, the micro-station is considered rigid, and only the nano-hexapod is considered with:

– 1dof actuators, $k=1\text{N}/\text{um}$, without parallel stiffness to the force sensors

- The bending stiffness of all joints are varied and the dynamics is identified

HAC plant (transfer function from f to dL , as measured by the external metrology):

- It increase the coupling at low frequency, but is kept to small values for realistic values of the bending stiffness (Figure 3.2a)
- Bending stiffness does not impact significantly the HAC plant. The added stiffness increases the frequency of the suspension modes Condition in [8] to have forces aligned with the struts when considering rotational stiffness: $k_r \gg k^* l^2$ For the current nano hexapod configuration, it correspond to $\gg 9000 \text{ Nm/rad}$. This may be an issue for soft nano-hexapod (for instance $k = 1e4 = l \gg 90$) = l have to design very soft flexible joints. Here, having relatively stiff actuators render this condition easier to achieve.

IFF Plant:

- Having bending stiffness adds complex conjugate zero at low frequency (Figure 3.2b)
- Similar to having a stiffness in parallel to the struts (i.e., to the force sensor). This can be explained since even if the force sensor is removed (i.e. zero axial stiffness of the strut), the strut will still act as a spring between the mobile and fixed plates because of the bending stiffness of the flexible joints. The frequency of the zero gives an idea of the stiffness contribution of the flexible joint bending stiffness
- They therefore impose limitation for decentralized IFF, as discussed in [10]
- This can be seen in the root locus plot of Figure 3.3a

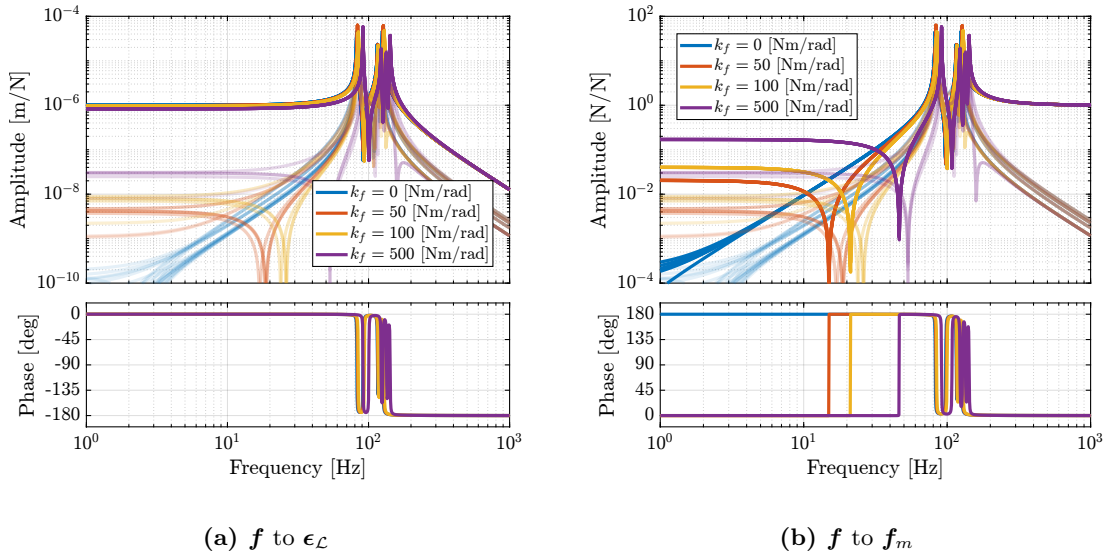


Figure 3.2: Effect of bending stiffness of the flexible joints on the plant dynamics. Both from actuator force f to strut motion measured by external metrology ϵ_L (a) and to the force sensors f_m (b)

However, as the APA300ML was chosen for the actuator, stiffness are already present in parallel to the

force sensors:

- The dynamics is computed again for all considered values of the bending stiffnesses with the 2DoF model of the APA300ML
- Root locus for decentralized IFF are shown in Figure 3.3b. Now the effect of bending stiffness has little effect on the attainable damping, as its contribution as “parallel stiffness” is small compared to the parallel stiffness already present in the APA300ML.

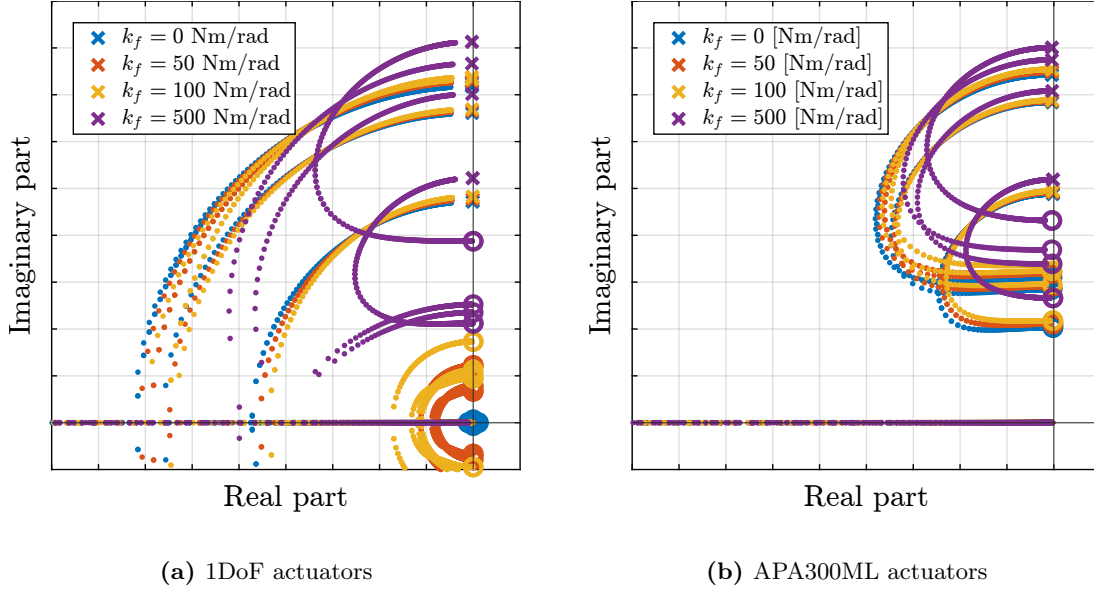


Figure 3.3: Effect of bending stiffness of the flexible joints on the attainable damping with decentralized IFF. When having an actuator modelled as 1DoF without parallel stiffness to the force sensor (a), and with the 2DoF model of the APA300ML (b)

Conclusion:

- Similar results for torsional stiffness, but less important
- thanks to the use of the APA, the requirements in terms of bending stiffness are less stringent

3.3 Axial Stiffness

- Adding flexibility between the actuation point and the measurement point / point of interest is always detrimental for the control performances. This is verified, and the goal is to estimate the minimum axial stiffness that the flexible joints should have
- Here, the mass of the strut should be considered. It is set to 112g as specified in the APA300ML specification sheet.
- Transfer functions are estimated for several axial stiffnesses (Figure 3.4)
- IFF plant is not much affected (Figure 3.4b). Confirmed by the root locus plot of Figure 3.5a

- “HAC” plant:
 - Additional modes at high frequency corresponding to internal modes of the struts. It adds coupling to the plant. This is confirmed by computed the RGA-number for the damped plant (i.e. after applying decentralized IFF) in Figure 3.5b

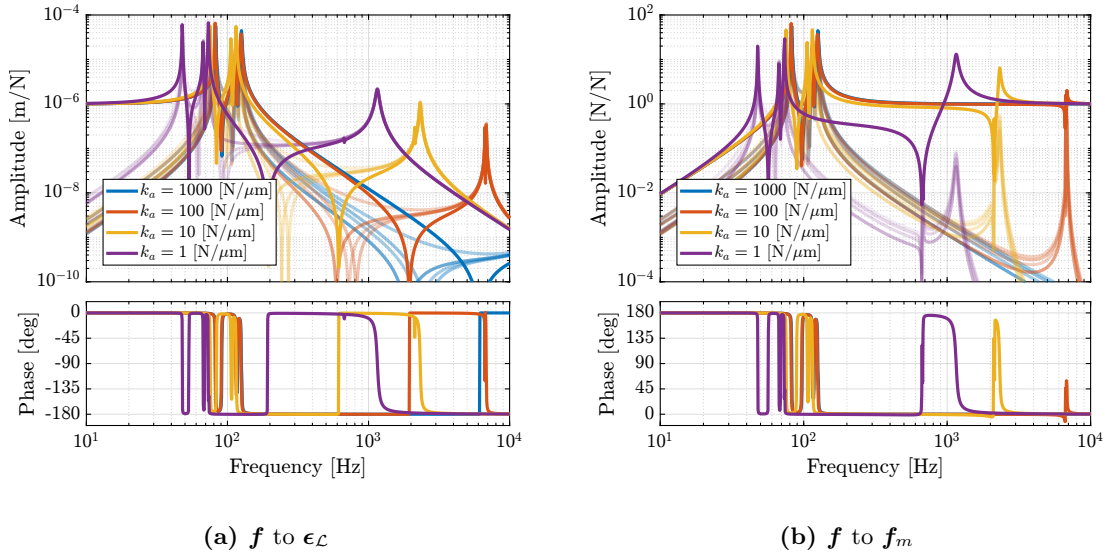


Figure 3.4: Effect of axial stiffness of the flexible joints on the plant dynamics. Both from actuator force f to strut motion measured by external metrology $\epsilon_{\mathcal{L}}$ (a) and to the force sensors f_m (b)

Integral force feedback

Maybe show the damped plants instead?

Root Locus: not a lot of effect

Conclusion:

- The axial stiffness of the flexible joints should be maximized to limit additional coupling at high frequency that may negatively impact the achievable bandwidth
- It should be much higher than the stiffness of the actuator
- For the nano-hexapod 100N/ μm is a reasonable axial stiffness specification
- Above the resonance frequency linked to the limited axial stiffness of the flexible joint, the system becomes coupled and impossible to control
- Also, loose control authority at the frequency of the zero

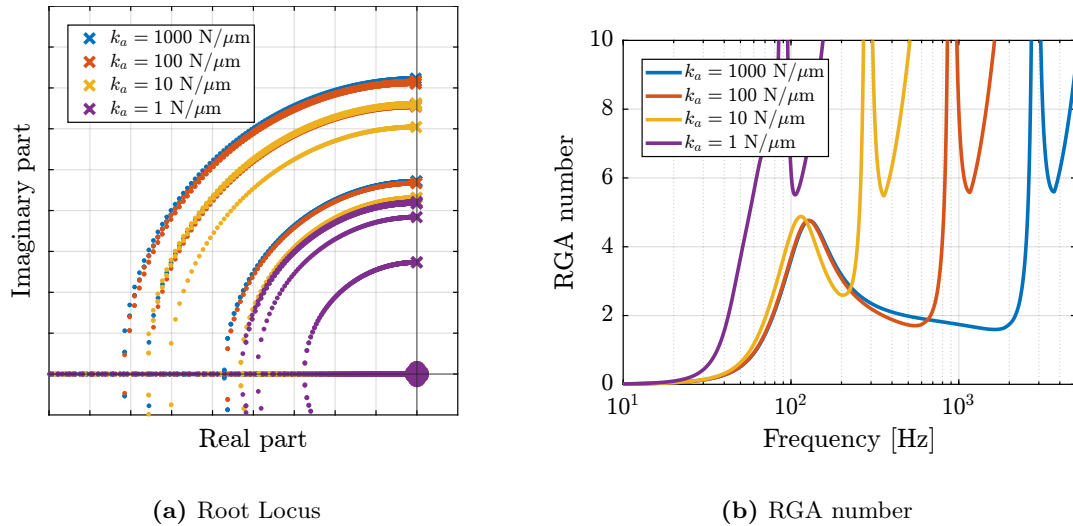


Figure 3.5: Effect of axial stiffness of the flexible joints on the attainable damping with decentralized IFF (a). Estimation of the coupling of the damped plants using the RGA-number (b)

3.4 Obtained design / Specifications

- Summary of specifications (Table 3.1)
- Explain choice of geometry:
 - x and y rotations are coincident
 - stiffness can be easily tuned
 - high axial stiffness
- Explain how it is optimized:
 - Extract stiffnesses from FEM
 - Parameterized model in the FE software
 - Quick optimization: (few iterations, could probably increase more the axial stiffness)
 - * There is a trade off between high axial stiffness and low bending/torsion stiffness
 - * Also check the yield strength
- Show obtained geometry Figure 3.6:
 - “neck” size: 0.25mm
- Characteristics of the flexible joints obtained from FEA are summarized in Table 3.1

Table 3.1: Specifications for the flexible joints and estimated characteristics from the Finite Element Model

	Specification	FEM
Axial Stiffness k_a	$> 100 N/\mu m$	94
Shear Stiffness k_s	$> 1 N/\mu m$	13
Bending Stiffness k_f	$< 100 Nm/rad$	5
Torsion Stiffness k_t	$< 500 Nm/rad$	260
Bending Stroke	$> 1 mrad$	24.5

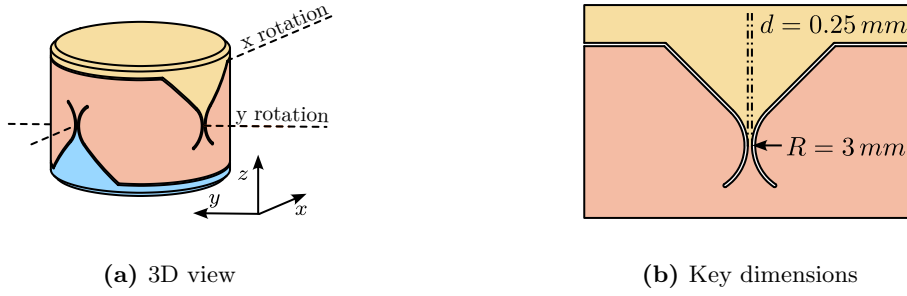


Figure 3.6: Designed flexible joints.

3.5 Validation with the Nano-Hexapod

To validate the designed flexible joint:

- FEM: modal reduction two interface frames are defined (Figure 3.7)
- additional 6 modes are extracted: size of reduced order mass and stiffness matrices: 18×18
- Imported in the multi-body model
- The transfer functions from forces and torques applied between frames $\{F\}$ and $\{M\}$ to the relative displacement/rotations of the two frames is extracted.
- The stiffness characteristics of the flexible joint is estimated from the low frequency gain of the obtained transfer functions. Same values are obtained with the reduced order model and the FEM.

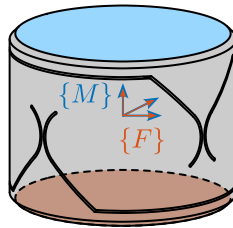


Figure 3.7: Defined frames for the reduced order flexible body. The two flat interfaces are considered rigid, and are linked to the two frames $\{F\}$ and $\{M\}$ both located at the center of the rotation.

Depending on which characteristic of the flexible joint is to be modelled, several DoFs can be taken into account:

- 2DoF (universal joint) k_f
- 3DoF (spherical joint) taking into account torsion k_f, k_t
- 2DoF + axial stiffness k_f, k_a
- 3DoF + axial stiffness k_f, k_t, k_a
- 6DoF (“bushing joint”) k_f, k_t, k_a, k_s

Adding more degrees of freedom:

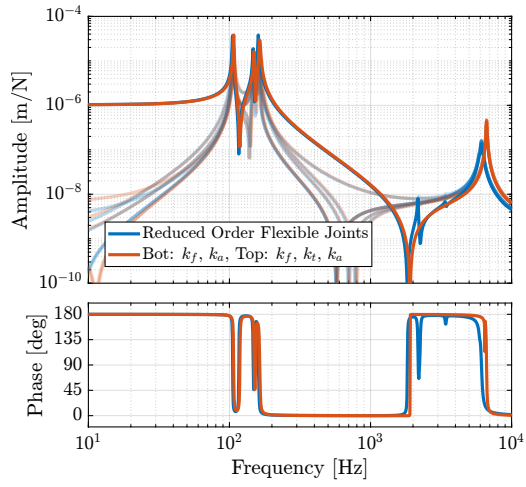
- can represent important features
- adds model states that may not be relevant for the dynamics, and may complexity the simulations without adding much information

After testing different configurations, a good compromise was found for the modelling of the nano-hexapod flexible joints:

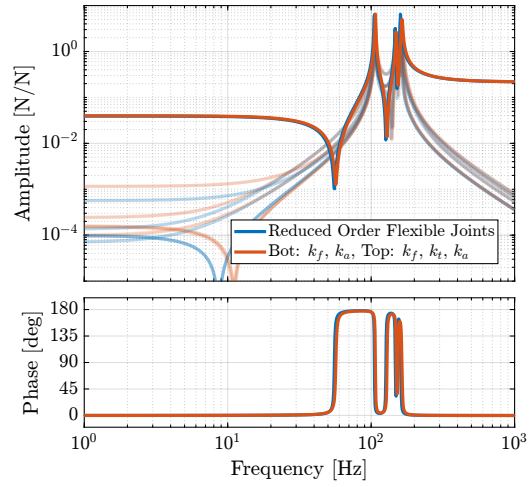
- bottom joints: k_f and k_a
- top joints: k_f, k_t and k_a

Talk about model order:

- with flexible joints: 252 states:
 - 12 for the payload (6 dof)
 - 12 for the 2DoF struts
 - 216 DoF for the flexible joints ($18*6*2$)
 - 12 states for?
- with 3dof and 4dof: 48 states
 - 12 for the payload (6 dof)
 - 12 for the 2DoF struts
 - 12 states for the bottom joints
 - 12 states for the top joints



(a) f to $\epsilon_{\mathcal{L}}$



(b) f to f_m

Figure 3.8: Comparison of the dynamics obtained between a nano-hexpod including joints modelled with FEM and a nano-hexapod having bottom joint modelled by bending stiffness k_f and axial stiffness k_a and top joints modelled by bending stiffness k_f , torsion stiffness k_t and axial stiffness k_a . Both from actuator force f to strut motion measured by external metrology $\epsilon_{\mathcal{L}}$ (b) and to the force sensors f_m (a).

Conclusion

Bibliography

- [1] A. M. Rankers, “Machine dynamics in mechatronic systems: An engineering approach,” Ph.D. dissertation, University of Twente, 1998 (cit. on p. 4).
- [2] M. R. Hatch, *Vibration simulation using MATLAB and ANSYS*. CRC Press, 2000 (cit. on p. 4).
- [3] F. Claeysen, R. L. Letty, F. Barillot, and O. Sosnicki, “Amplified piezoelectric actuators: Static & dynamic applications,” *Ferroelectrics*, vol. 351, no. 1, pp. 3–14, 2007 (cit. on p. 5).
- [4] A. J. Fleming and K. K. Leang, *Design, Modeling and Control of Nanopositioning Systems* (Advances in Industrial Control). Springer International Publishing, 2014 (cit. on p. 7).
- [5] A. J. Fleming and K. K. Leang, “Integrated strain and force feedback for high-performance control of piezoelectric actuators,” *Sensors and Actuators A: Physical*, vol. 161, no. 1-2, pp. 256–265, 2010 (cit. on p. 7).
- [6] A. A. Hanieh, “Active isolation and damping of vibrations via stewart platform,” Ph.D. dissertation, Université Libre de Bruxelles, Brussels, Belgium, 2003 (cit. on p. 13).
- [7] A. Souleille, T. Lampert, V. Lafarga, *et al.*, “A concept of active mount for space applications,” *CEAS Space Journal*, vol. 10, no. 2, pp. 157–165, 2018 (cit. on p. 16).
- [8] J. McInroy, “Modeling and design of flexure jointed stewart platforms for control purposes,” *IEEE/ASME Transactions on Mechatronics*, vol. 7, no. 1, pp. 95–99, 2002 (cit. on pp. 21, 23).
- [9] X. Yang, H. Wu, B. Chen, S. Kang, and S. Cheng, “Dynamic modeling and decoupled control of a flexible stewart platform for vibration isolation,” *Journal of Sound and Vibration*, vol. 439, pp. 398–412, Jan. 2019 (cit. on p. 22).
- [10] A. Preumont, M. Horodinca, I. Romanescu, *et al.*, “A six-axis single-stage active vibration isolator based on stewart platform,” *Journal of Sound and Vibration*, vol. 300, no. 3-5, pp. 644–661, 2007 (cit. on pp. 22, 23).
- [11] Z. Du, R. Shi, and W. Dong, “A piezo-actuated high-precision flexible parallel pointing mechanism: Conceptual design, development, and experiments,” *IEEE Transactions on Robotics*, vol. 30, no. 1, pp. 131–137, 2014 (cit. on p. 22).